scientific reports

Check for updates

OPEN

Distinct pathway of multiferroic silver-decorated zinc ferrite nanocatalyst performance for Acinate insecticide oxidation

Hossam A. Nabwey[1,2]✉ & Maha A. Tony[2,3]

The current study investigating the preparation and application of a Multiferroic nano-scale silver zinc ferrite substance ($Ag_{0.5}Zn_{0.5}Fe_2O_4$ nanocatalyst) has been established. Multiferroic silver zinc ferrite substance is prepared by co-precipitation technique as hybridized composite. This synethsized nanoparticles was characterized via X-ray diffraction (XRD), high-resolution transmission electron microscopy (HRTEM) as well as Scanning Electron Miscospopy (SEM). Such nanoparticles are used as a sustainable recyclable photo-Fenton's reagent precursor for treating insecticide in wastewater. The results revealed a high Acinate oxidation rate reached to 97% removal within 40 min of irradiance time. To increase the performance, the operating variables are optimized. pH 3.0 and 40 and 400 mg/L for $Ag_{0.5}Zn_{0.5}Fe_2O_4$ and hydrogen peroxide, respectively are identified as the optimum values. Also, kinetics and thermodynamic are evaluated and the reaction is subsequent the first-order kinetics model and exothermic and non-spontaneous in nature with a low energy barrier of 35.02 kJ/mol. The advantage of $Ag_{0.5}Zn_{0.5}Fe_2O_4$ catalyst is its sustainability since it recovered for multiple reuse with a high activity reached to 80% removal rate after six cyclic use compared to 97% of fresh catalyst use.

Keywords Oxidation, Fenton reaction, Insecticide, Wastewater, Photocatalyst, Nanomaterial

Although, water is a vital resource, the progressive in modernization and various human activities are causing its insufficiencies[1,2]. By the year 2050, estimation projected the water utilization and consumption is in increase to about 20–30% compared to the present era. Such estimate is associated to the populous, economic and technological development of the modern societies that means water pattern is in decline[3–5]. Industry is signified as the big water consumption sector worldwide, which expends massive amounts of water while the whole water consumed in such sector represents nearly 20% of the entire consumed amount[6]. Vast amounts of water is consumed though agriculture activities. The result is watercourses pollution through the overuse of chemical fertilizers and insecticides. Moreover, such chemicals discharge causes a deterioration into the aquatic system[7,8]. Safeguarding the aquatic ecosystem is critical in order to assure a sustainable existence. Thereby, the remediation of such effluents prior to its ultimate discharge is essential and attaining a dispute for environmental sector as well as the academic researchers to meet the environmental protocols. But, the chemicals used including pesticides are difficult to degrade[3,8].

Up to now, numerous methods of treatment are suggested for such pollutants' elimination scheme. Such technologies are including biological[9], chemical[10,11], and physical[12] techniques. Nevertheless, chemical treatment is signified as most appropriate scheme. Adsorption[13–15], catalytic oxidation[16–18] and ultraviolet/solar catalysis[19] revealed reasonable treatments. Remarkably, advanced oxidation processes (AOPs) that are indicated as an emerging chemical oxidation field is achieving a noteworthy scientists' attention as a green choice[20]. In such treatments either heterogeneous or homogeneous mixture are used as an oxidizing agent and transition metal. It is noteworthy to mention that, Fenton, Fenton-like and photo-Fenton method that combines iron with H_2O_2 is gaining a special attention. However, the presence of the used catalyst in the final discharge is a challenge for real application due to the existence of the secondary pollutant[21–24]. However, the techniques generally applied to separate such nanoparticles, i.e. filtration and centrifugation may be signified as an issue due to their time-

[1]Department of Mathematics, College of Science and Humanities in Al-Kharj, Prince Sattam bin Abdulaziz University, Al-Kharj 11942, Saudi Arabia. [2]Basic Engineering Science Department, Faculty of Engineering, Menoufia University, Shebin El-Kom 32511, Egypt. [3]Advanced Materials/Solar Energy and Environmental Sustainability (AMSEES) Laboratory, Faculty of Engineering, Menoufia University, Shebin El-Kom 32511, Egypt. ✉email: eng_hossam21@yahoo.com

consuming nature and potential to interrupt the system. in this regard, it is noteworthy to mention that magnetic nanocatalysts can be used to address these issues. Magnetic nanocatalysts posses some merits including simplicity in preparation, low toxicity, good chemical stability, straightforward separation via magnetic field application in the absence of chemicals, cost-efficient materials, and ultimate recovery in a simple manner[25–27]. Thereby, the selection of a sustainable catalyst is a must. In respect to the green chemistry principle, developing non-toxic, cost-efficient, and recyclable and easily handling catalyst from reaction is a suitable candidate to overcome such drawback.

Several attempts have been published to develop nanoparticles that could be participating in green chemistry since it could be recycled from the reaction media[28–30]. In this context, ferrite nanoparticles is a suitable candidate and their magnetic activity makes them applied in vast industrial applications. Ferrites material are technically valued since they posses high magnetic permeability[31–33] with minimal losses after use[13,34,35]. Also,At low substrate pH, the such materials are thermally and chemically stable in aqueous media[36,37]. Additionally, the low band gap of ferrites when compared with some semiconductors is achieving the merit of being proficient in absorbing a part of the so-called visible light[38–40]. Accordingly, research studies by academia are focused on exploring appropriate ferrite nanoparticles with their merits for saving the aquatic pollution. Consequently, searching for innovative multifunctional materials as a photocatalyst is attaining the researchers' attention. Multiferroic substances are defined as materials that exhibit more than one of the primary ferroic properties in the same phase signified as a multifunctional substances posses simultaneous effects of ferroic properties such as ferroelectricity, ferromagnetism, ferroelasticity, etc[41,42]. Also, the Multiferroic composite gains its importance due to it could exhibits spontaneous polarization upon illumination by light irradiation, causing an imbalance of charges, thereby inducing a strong internal electric field leading to separation of charges[43,44]. Such charges are responsible of redox reactions that are essential for catalytic oxidation. The photocatalytic properties of the multiferroics substances have been a motivation for researchers to apply such materials in potential candidate for environmental applications[45–47]. However, limited research is applied using such materials as a photocatalyst especially for agriculture waste effluent[48–50]. Hence, further studies are essential to validate their real use as an eco-friendly oxidative scheme. Nevertheless, conferring to the background of the authors' knowledge that is achieved according to the literature published, there is a deficiency in research articles cited from published articles for applying Ag@Zn-ferrites as a precursor of super paramagnetic Fenton's photocatalyst for eliminating Acinate insecticide.

In line of sustainable environment introducing Ag@Zn-ferrites as a source of Fenton's catalyst is assessed. Consequently, the prepared substance are characterized using X-ray diffraction (XRD), scanning electron microscope (SEM) and the transmission electron microscopy (TEM) images, which verified the presence of composite nanoparticles. The scheme is applied for oxidizing Acinate insecticide through the use of ultraviolet Muliferroic-Fenton reaction. The reaction operational parameters are explored and the optimized conditions are supported.

Experimental investigation

Synthesis of multiferroic nanocatalyst

Iron nitrates (purity of ≥ 99.94%), silver nitrate and zinc nitrate hexahydrate (≥ 99.8%) are used as the precursors for ferrites nanoparticles preparation and all purchased from Sigma Aldrich. Also, sodium hydroxide (99.0%) is used for the Ag@Zn-ferrites composite precipitation. Particularly, the chemicals used are of analytical grade and tested and applied as attained with no extra treatment or further purification.

Multiferroic $Ag_{0.5}Zn_{0.5}Fe_2O_4$ nanocatalyst was synthesized by using co-precipitation routine. Aqueous media matrix of starting precursors $Fe(NO_3)_3{\cdot}9H_2O$, $Ag(NO_3)_3$ and $Zn(NO_3)_2{\cdot}6H_2O$ in their stoichiometric ratio and all of them are used as received. Thus, following the molar contents of ferrite the stoichiometric compositions of percoursers are calculated and the essential fractions were added then the solution was magnetically stirred to achieve homogeneity. Afterwards, at the mean time, droplets of ammonia solution was supplemented to increase the pH value to about 12 while the solution is exposed for heating at about 80 °C to initiate the nanoparticles formation.

The attained precipitate is collected, which is successively washed to lessen the pH to neutral (~ 7.0) and thereby the powder is dried in an electrical oven drying through heating under 80 °C overnight (about 12 h). Afterwards the attained particles are dried out prior to ground retaining agate mortar and pestle to achieve fine powder of Multiferroic nanocatalyst. Then, the resulting powder is integrated as a Fenton-Multiferroic nanocatalyst.

Acinate photocatalytic oxidation test

Commercial grade Acinate ($C_5H_{10}N_2O_2S$) insecticide, (90% concentration) is purchased from central agricultural pesticide and Chemicals Company in Egypt. Acinate insecticide is applied as the source of simulated agriculture waste effluent. Primarily, 1000-ppm Acinate aqueous solution is prepared as a stock aqueous solution while a successive dilution is done, when required. Furthermore, the pH of the Acinate insecticide wastewater was regulated, if needed, to certain values by adding sulphuric or sodium hydroxide (supplied by Sigma-Aldrich) using a digital type pH meter (model, AD1030, supplied by Adwa instrument, Hungary). Hydrogen peroxide, H_2O_2, with a concentration of 30% w/v reagent was used to introduce the catalyst Ag@ZnFerrite catalyst. Both reagents are the precursor of Fenton's oxidation reaction system test.

To conduct the photocatalytic oxidation test, a jar test is prepared by pouring 100-mL of Acinate solution at a certain dosing into a glass vessel for the object of investigating the effect of Acinate dose on the Fenton's oxidation. Also, pH is adjusted, if required, to the desired values using digital pH-meter (AD1030, Adwa instrument, Hungary). Subsequent, Multiferroic silver decorated zinc ferrite nanocatalyst composite ($Ag_{0.5}Zn_{0.5}Fe_2O_4$) is added into the Acinate wastewater at a certain required concentration. Then, to well disperse the $Ag_{0.5}Zn_{0.5}Fe_2O_4$

catalyst, the mixture is exposed to ultrasonic dispersion through five minutes with no heat exposed. Following, the H_2O_2 at its required dose is added into the Acinate wastewater mixture.

Afterwards, to assure good dispersion for the mixture, all the heterogeneous solution is exposed to stirring during the ultraviolet irradiance. The ultraviolet emitted though a UV lamp with 253.7 nm wavelength (15 W, 230 V/50 Hz). Furthermore, the solution temperature effect is assessed nd the Fenton's reagent is initially added and thereafter the temperature is elevated. Subsequently, after treatments, the treated water is exposed for spectrophotometric analytical methodology at a certain time intervals. A UV-vis spectrophotometer (Unico, Model UV-2100, USA), was used to asses the residual Acinate in the solution at the absorbance of 231 nm. Finally, Chemical oxygen demand (COD) of the remediated wastewater effluent was analysed using Lovibond Checkit direct COD Photometer, supplied from Germany. All the runs are done in triplicate technique. Prior to the wastewater treated effluent subjected for analysis, the Multiferroic $Ag_{0.5}Zn_{0.5}Fe_2O_4$ nanocatalyst were removed using a micro-filter. The design of the experimental steps is shown in Fig. 1.

Characterization techniques

The phase structure of the organized $Ag_{0.5}Zn_{0.5}Fe_2O_4$ substance is verified via diffracted XRD, X-rays pattern model X-lab Shimadzu X-6000 X-ray diffractometer that is conducted under a scan step of 0.02° mode. Additionally, $Ag_{0.5}Zn_{0.5}Fe_2O_4$ substance morphology was investigated via scanning electron microscope (SEM) model Quanta FEJ20 and high resolution transmission electron microscopy (HRTEM) model Tecnai G20, FEI).

Results and discussions

Characterization of the composite material

XRD analysis

The powder X-ray diffraction (XRD) pattern of the produced $Ag_{0.5}Zn_{0.5}Fe_2O_4$ substance is exhibited in Fig. 2. As displayed in the figure, XRD graph exposes the presence of sharp peaks indicate the occurrence of the crystalline structure of ferrites. JCPDS reported that 591–0028 and 153–9598 are the diffraction peaks equivalent to the cubic spinel structure The substance allocated as displayed in Fig. 2 that appointed with the lattice planes [220], [311], [222], [400] and [511] that corresponding to the diffraction peaks (2θ) of 30.69, 34.06, 37.16, 43.57 and 57.20, respectively that reflects the presence of zinc ferrites. The spinel phase's elaboration is displayed as the uppermost strong peak of 2θ 34.6, which is visible at the plane of [311]. Other prominent peaks of zinc ferrite and their signified planes are well recognized. Also, the sample showed high crystalline in nature according to

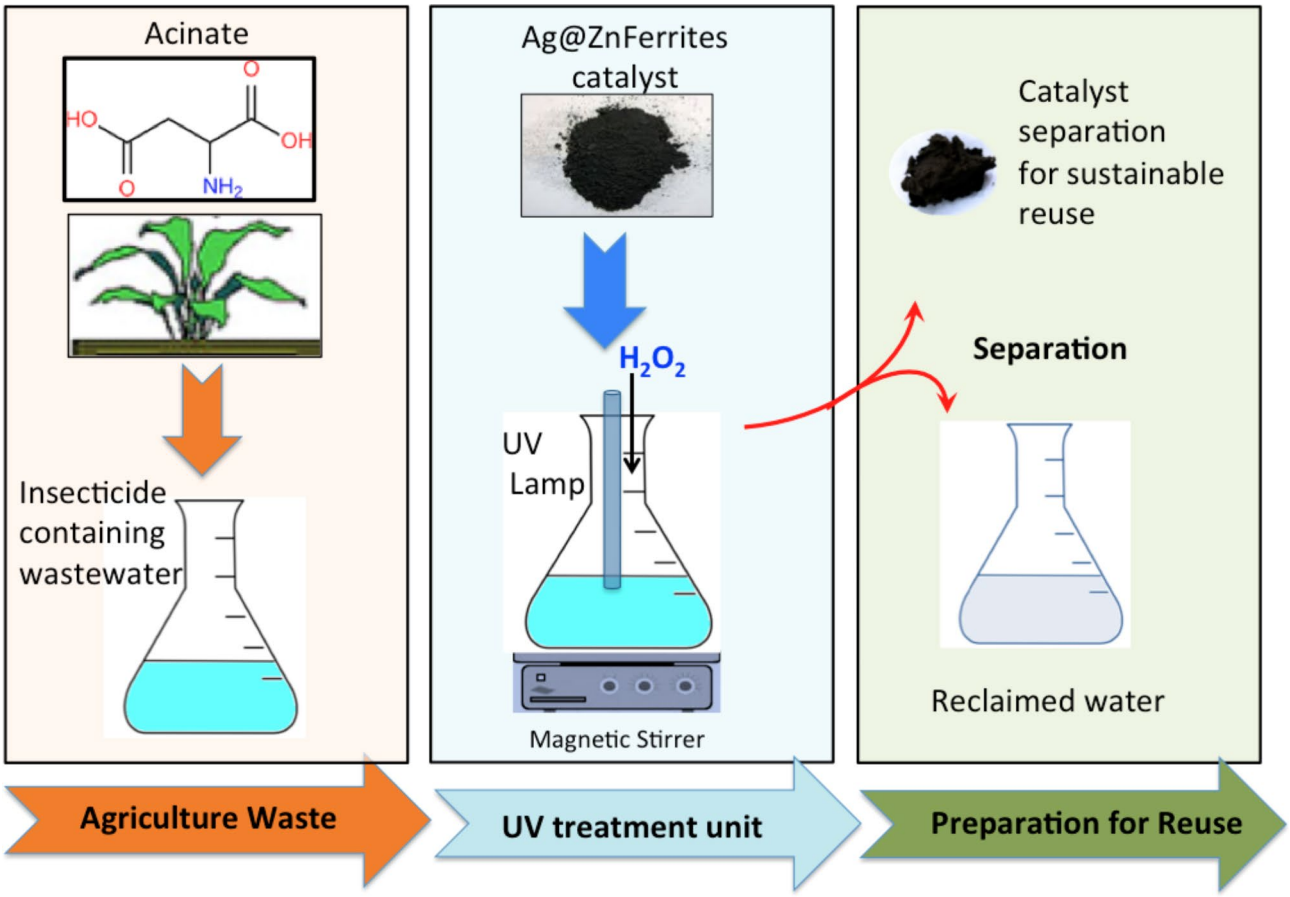

Fig. 1. Graphical design of the treatment steps.

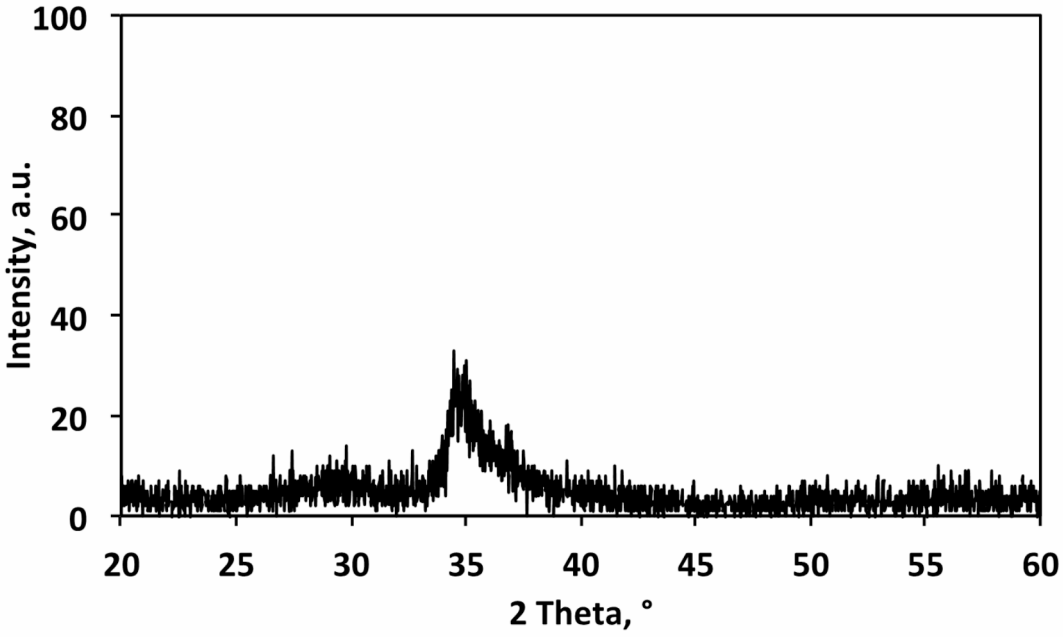

Fig. 2. XRD pattern of $Ag_{0.5}Zn_{0.5}Fe_2O_4$ nanoparticles.

the XDR pattern. The presence of two low intensive peaks at 38.4 and 44.6 signifies the planes of [111] and [200] of silver[39]. This, in turn, confirms the presence of the Multiferrioc material, silver-zinc ferities.

The crystallite size (d) of $Ag_{0.5}Zn_{0.5}Fe_2O_4$ nanoparticles was determined using the Scherrer equation ($d = \frac{k\lambda}{\beta cos\theta}$)[42], at the angle of diffraction (θ) of the high-intensity peak [311], where (k) is the Scherrer constant and (λ) is the X-ray wavelength.

SEM micrographs

$Ag_{0.5}Zn_{0.5}Fe_2O_4$ material is characterized though investigating its morphology. The surface morphology is evaluated through scanning electron microscope (SEM) investigation and the micrographs are given in Fig. 3. As exhibited in the micrographs, agglomerated nanoparticles is displayed at the surface of ferrites with mixed shapes including spherical morphology and mixed sheets of such nanoparticles. $Ag_{0.5}Zn_{0.5}Fe_2O_4$ nanoparticles are indicated as spherical, sheets and mixed shapes particles with a narrow grain size distribution.

TEM images

For the object of well examines the morphology of the substance, high resolution transmission electron microscopy (HRTEM) analysis is carried out. The micrographs in Fig. 4a and b in different magnification exhibited a semi-spherical nanoparticles of $Ag_{0.5}Zn_{0.5}Fe_2O_4$ substance as decorated ferrites. According to image of Fig. 4b displayed as a specific nanoparticle displayed as semi-spheres. It is noteworthy to mention that, TEM micrograph illustrates the accumulation of polygonal silver ferrite layer supported a tetragonal zinc oxide nanocrystals.

Effectiveness of Acinate oxidation

Effect of oxidation time and comparative different systems

The effectiveness of reaction time the catalytic oxidation of Acinate insecticide from wastewater effluent has been explored. In this regard, the outcomes of oxidation time using Multiferroic $Ag_{0.5}Zn_{0.5}Fe_2O_4$ /H_2O_2; Multiferroic/H_2O_2/UV and H_2O_2/UV oxidation schemes were assessed to investigate the experimental parameters for the further experimental study. The effectiveness of such oxidation methodologies was evaluated in the terms of Acinate concentration and Chemical Oxygen Demand (COD) elimination and reduction.

Initially, the as-prepared Multiferroic substance was injected into the aqueous mixture at either its natural pH (6.2) and pH (3.0). Then, the reaction was initiated by adding 400 mg/L of hydrogen peroxide for the Dark Fenton reaction oxidation system. The data exhibited in Fig. 5a and b validate that both Acinate concentration and Chemical Oxygen Demand (COD) removals are higher when the pH of effluent is monitored at acidic pH 3.0 value.

The Acinate insecticide removal efficacy extended to only 96% and 87% for Acinate removal and COD reduction, respectively. Thus, it is obvious from the data comparison that explored in Fig. 5a and b that the

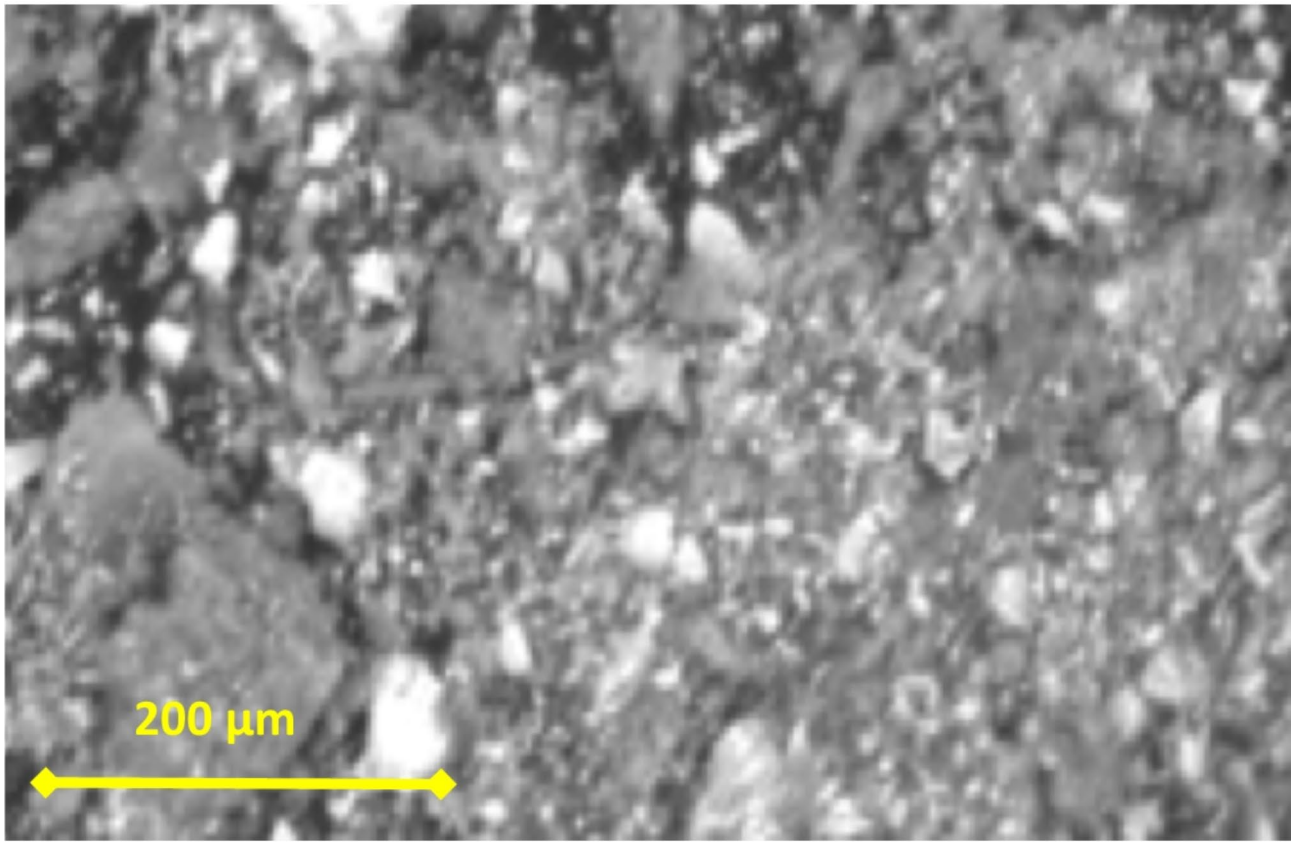

Fig. 3. SEM images of the $Ag_{0.5}Zn_{0.5}Fe_2O_4$ nanoparticles composite material.

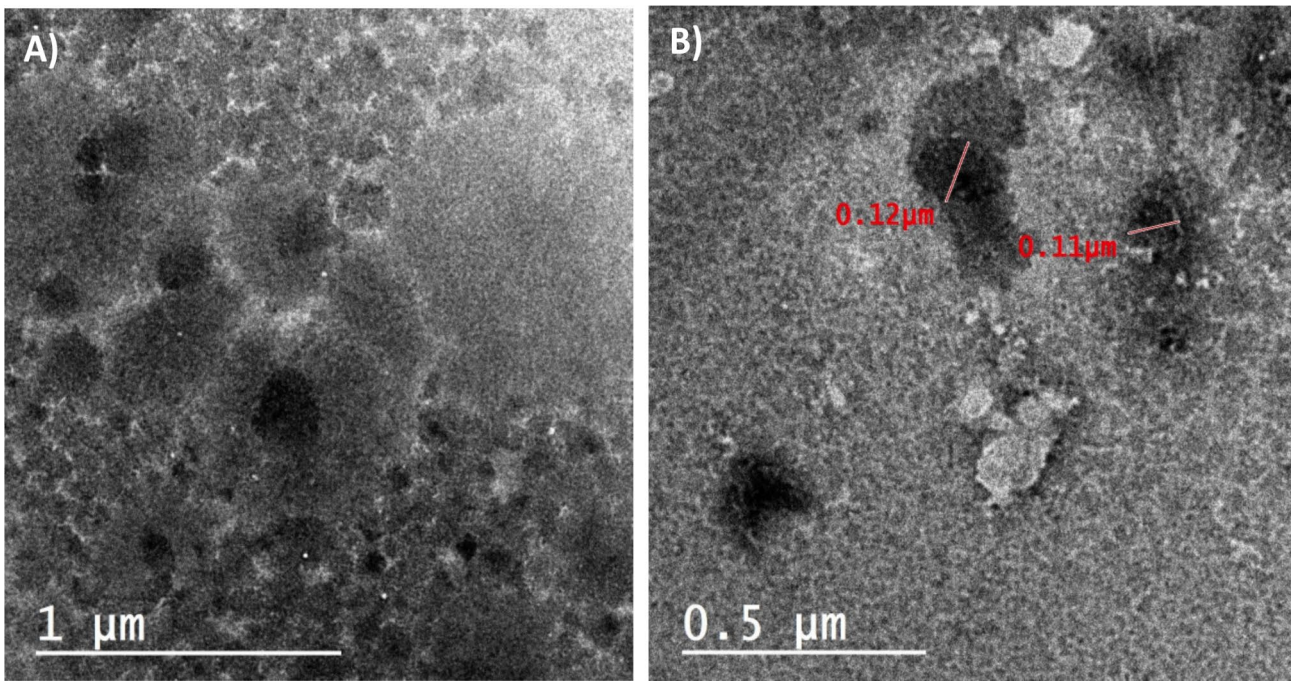

Fig. 4. TEM images at different magnification of the $Ag_{0.5}Zn_{0.5}Fe_2O_4$ composite substance.

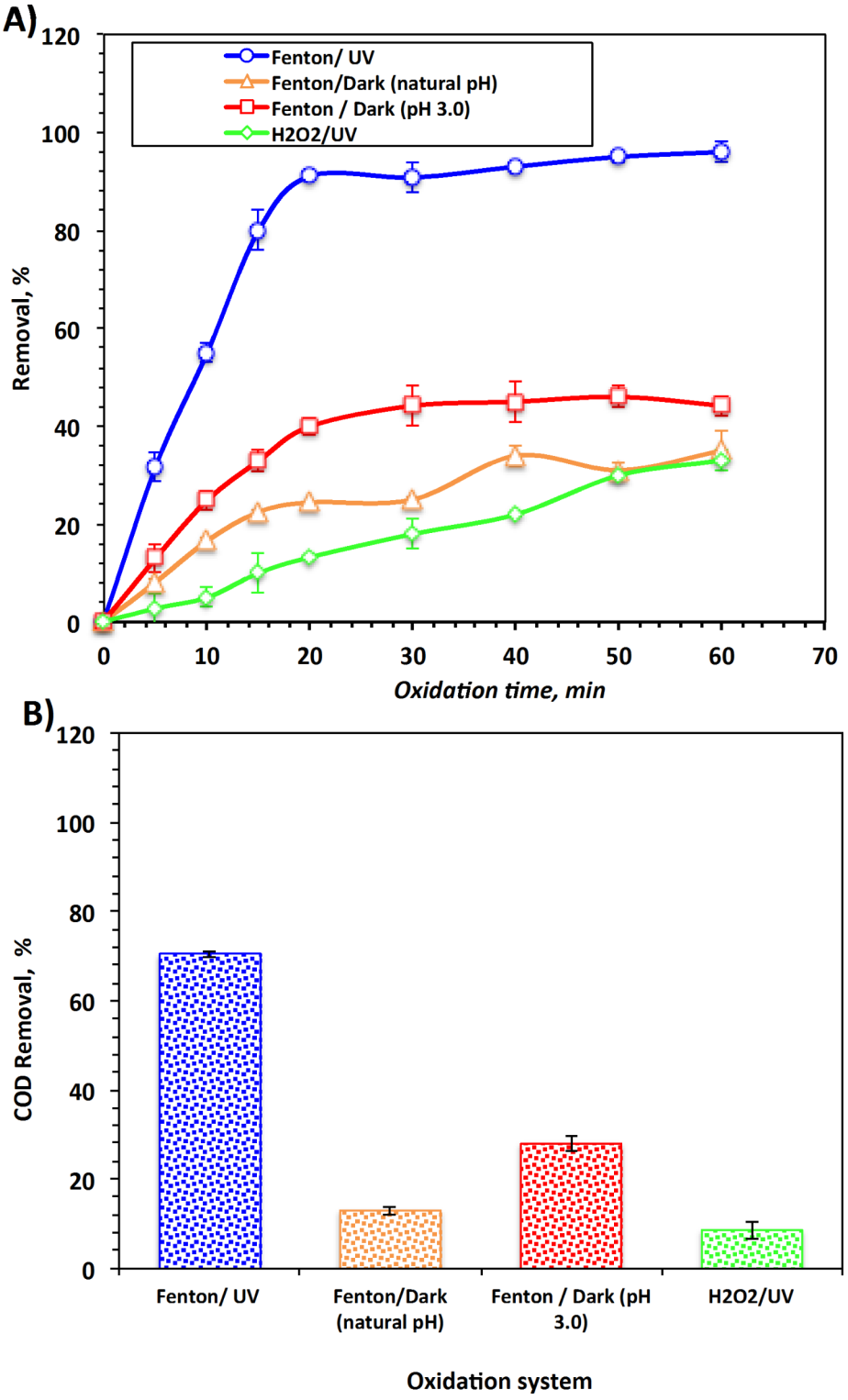

Fig. 5. Effect of reaction time on multiferroic-Fenton system and comapred with other oxidation systems.

ultraviolet irradiance illumination is an efficient tool for pristine hydrogen peroxide oxidation reaction system or photo-Fenton system as the reduction is more advanced when compared to the dark reaction test. However, this is reduced to only 44% and 26% for Acinate and COD_S' removals, respectively in a dark reaction system of oxidation. It is significant to remark that for the object of comparison, when pH is not in acidic medium specially pH 3.0, the removal are declined. A quick oxidation reaction tendency in the preliminary stage of reaction is signified for all the Fenton reaction and H_2O_2 oxidation. Fenton reaction oxidation system is occurred using the activation of hydrogen peroxide with iron salt for hydroxyl radical ($^{\cdot}OH$) generation. However, such test

is incremented under the ultraviolet irradiance since extra OH radicals are generated. It is noticeable, with prolonging of time, the removal rate is slowed down and the efficiency became stabilized. This rapid oxidation rate in the initial stage for the oxidation is also linked to the ˙OH radicals generated. Those radicals are radicals are the main reliable of the Acinate oxidation. However, with the time exceeds, the overall hydroxyl (˙OH) radicals generated is deduced. Such radicals are gradually declined with the exceeding of time, corresponding to the reduction in the hydrogen peroxide concentration after the preliminary oxidation time with the formation of other radicals that hinders the reaction rate rather than increasing the pollutant oxidation[23,43]. Furthermore, extra radicals are generated in the reaction media and the oxidation develops more complex. Such radicals produced in that case are namely hydroperoxyl radicals (HO_2) that reduce the oxidation reaction system with the time proceeding. Hence, those radicals reduce the oxidation of Acinate rather than eliminating them through oxidation[40].

In the pristine hydrogen peroxide oxidation scheme, with the time prolonging, the reagent is spent and thereby, the Acinate reduction tendency is declined. As previously stated in the aforementioned studies in literate[31,51–55], various work demonstrated such trend on the oxidation reaction tendency, which is greater at the preliminary oxidation time and deduced whereas the reaction progresses. This could be attributed by the ˙OH radicals' generation, which is in excess elevated at the initial period. While the same rapid preliminary oxidation of Acinate affinity happens in the preliminary stage of all the Fenton's oxidation, the removal is limited to only 13% for Acinate elimination using Dark Fenton system. This is associated with the occurrence of the UV radiation that admitting extra ˙OH generation and therefore the oxidation tendency is pronounced[56–58].

Effect of Acinate loading on multiferroic-Fenton oxidation system

For the object of reaching to a real scale application, it is essential to investigate various Acinate loading where initial insecticide concentration is varied. pH and concentrations of $Ag_{0.5}Zn_{0.5}Fe_2O_4$ and hydrogen peroxide are kept constant while the Acinate loading is varied a function to attain its effect under the UV illumination. The efficacy of such performances was estimated in terms of diverse Acinate concentrations varied from 20 to 100 mg/L at pH value of acidic pH (3.0).

The data showed in Fig. 6 exposed that while all Acinate loading could be oxidized by the Multiferroic-Fenton oxidation system based on oxidation protocols, removal efficiency is varies according to the Acinate loads and the higher loading reduces the efficiency to reach to only 55% in comparison to a higher removal rate (97%) at low Acinate concentration (20 mg/L). This might be attributed to the hydroxyl (OH) radicals' generation. OH radicals outlined throughout the catalytic decay of H_2O_2 reagent by the catalyst nanocomposite substance[35]. Such trend might be linked to the H_2O_2 and Multiferroic $Ag_{0.5}Zn_{0.5}Fe_2O_4$ catalyst are the same although the Acinate loading is elevated that means the produced hydroxyl radicals are not sufficient for oxidizing pollutant molecules. Correspondingly, it is notable to declare that increment removal efficacy is achieved through the preliminary reaction time for all the Acinate dose systems. Furthermore, while $Ag_{0.5}Zn_{0.5}Fe_2O_4$ is beforehand suggested just an adsorbent material. Scattered researchers in the previous published articles[8,35] proposed it as a photocatalyst since its photocatalytic pursuit. Furthermore, the accessible active vacant sorbent spots on the $Ag_{0.5}Zn_{0.5}Fe_2O_4$ nanocomposite is not adequate to adsorb Acinate molecules[33]. Similar trend is achieved for the COD removal efficiency. It is also may be concluded that the higher concentrations of Acinate substance in the reaction medium results in further frequent production of by-products and intermediates that in turn leading to a deduction in Acinate oxidation rate[20]. Formerly reported literature confirmed such trend effect on rendering the catalytic activity since the pollutant is elevated in concentration and thereby the removal effectiveness falls[48–50].

Effect of hydrogen peroxide on multiferroic-Fenton oxidation

In the light of gaining the supreme Multiferroic-Fenton pursuit, it is important to attain the optimum H_2O_2 coexistence in the aqueous media. This concept is leading to the initiate the $Ag_{0.5}Zn_{0.5}Fe_2O_4$ catalyst of the Multiferroic-Fenton system with the complemented optimum concentration of hydrogen peroxide. Hence, the hydroxyl radicals (OH) are produced in its maximum efficiency. In this concept, primarily the combined reagent of H_2O_2 with $Ag_{0.5}Zn_{0.5}Fe_2O_4$ catalyst are altered in the range of 50 to 600 mg/L (at a constant acidic conditions pH (3.0) and $Ag_{0.5}Zn_{0.5}Fe_2O_4$ concentration of 40 mg/L), and the Acinate as well as the COD removal efficacy is assessed.

The data revealed in Fig. 7 exhibited that the hydrogen peroxide concentration elevation from 50 to 400 mg/L might improve the oxidation efficacy. Nevertheless, an opposed tendency is investigated with extra reagent increase reached to 600 mg/L. This phenomenon is linked to the key active catalytic specie in the photocatalytic reaction that is signified as OH radicals is associated with the optimal presence of hydrogen peroxide and catalyst occurrence[31,51]. This is leading to an enhancement and elevation in the photocatalytic Acinate elimination and reduction ability. Additionally, the superior photocatalytic opportunity with an increase in the oxidation yield is recorded its highest efficiency when the hydrogen peroxide is at the optimal concentration of 400 mg/L[52–54].

Effect of multiferroic nanocomposite loading

For economic and more efficient feasibility, it is essential to locate the optimal catalyst dose. In an effort to reach to the adjusted reagent dosing for the concept of fitting the application, the catalyst ($Ag_{0.5}Zn_{0.5}Fe_2O_4$) loading is examined on the implementation of the photocatalytic oxidation system. In this concept, the concentration of $Ag_{0.5}Zn_{0.5}Fe_2O_4$ nanocomposite is assessed to explore Multiferroic-Fenton oxidation tendency (Fig. 8). The data exposed in Fig. 8 exhibits the effect of the Fenton oxidation on varies $Ag_{0.5}Zn_{0.5}Fe_2O_4$ from 10 to 80 in the units of mg per litre, whereas, all other operational variables are kept constant (400 mg/L for H_2O_2 and pH of 3.0).

The maximal Acinate removal efficacy is recorded to its almost complete (97%) removals as well as highest COD removal of 92% when 40 mg/L of catalyst is applied as a precursor of Multiferroic-Fenton system. While

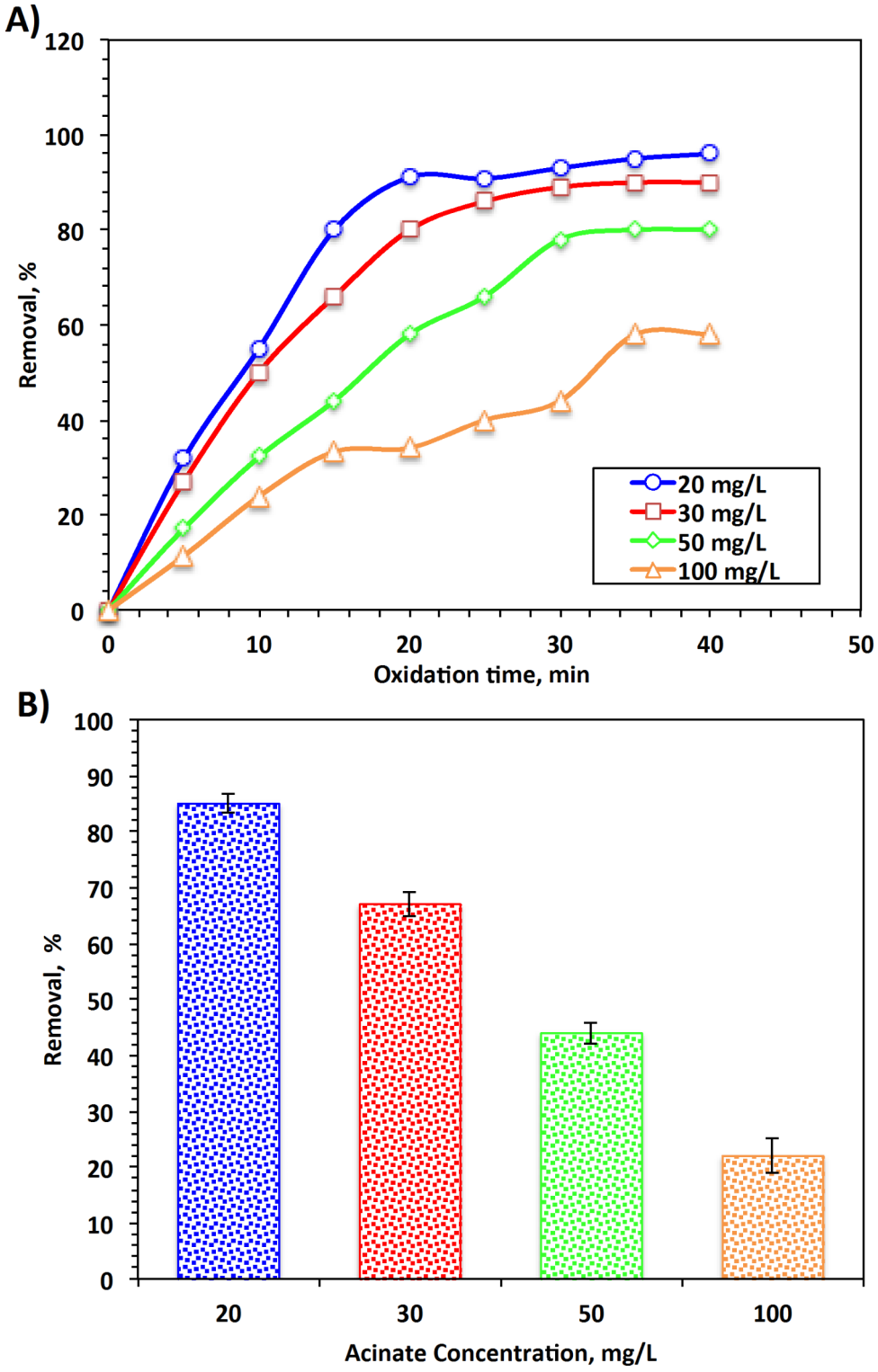

Fig. 6. The effect of Acinate loading on the multiferroic-Fenton oxidation ($Ag_{0.5}Zn_{0.5}Fe_2O_4$ 40 mg/L, H_2O_2 400 mg/L, pH 3.0).

it reached to 62, 79 and 90% removals within the reaction time of 40 min, respectively for the corresponding doses of 10, 20 and 80 mg/L of $Ag_{0.5}Zn_{0.5}Fe_2O_4$, respectively. This might be validated through the amount of H_2O_2 of 400 mg/L, which is constant in all cases. Consequently, the achieved yield of ·OH radicals produced is not adequate reaching to a complete Acinate oxidation. Such investigation-attained means the H_2O_2 should be in balance to expand the (·OH) radicals' generation and could not be lessen the effective ·OH radicals' quantity. A comparable investigation is previously stated and reported in varied study[34,55]. This could be attributed by

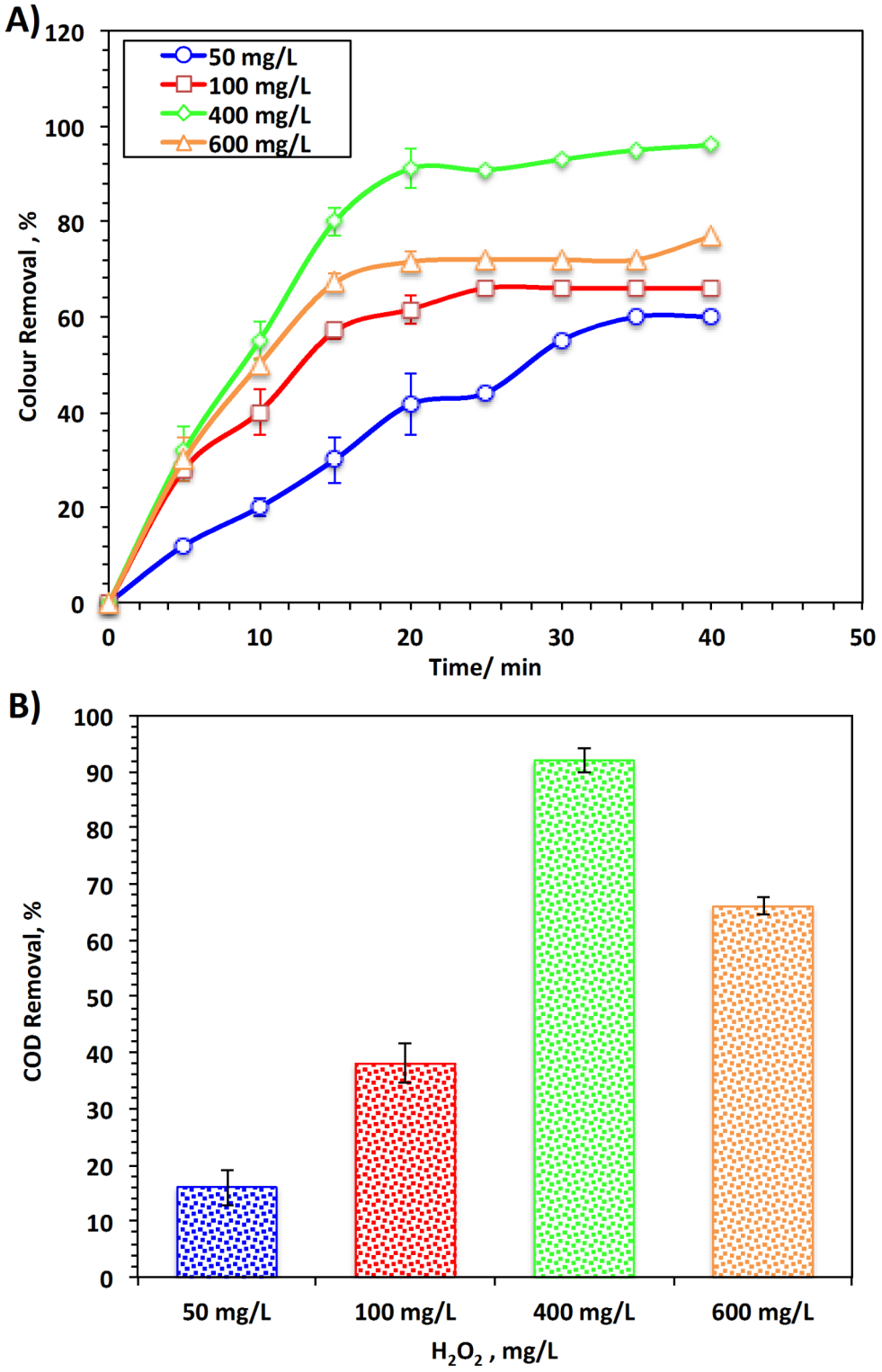

Fig. 7. Effect of hydrogen peroxide loading on multiferroic-Fenton oxidation based oxidative system ($Ag_{0.5}Zn_{0.5}Fe_2O_4$ 40 mg/L, pH 3.0).

increasing the $Ag_{0.5}Zn_{0.5}Fe_2O_4$ catalyst concentration to more than the optimum value might leading to the affinity of the catalyst particles to agglomerate, therbey, part of the $Ag_{0.5}Zn_{0.5}Fe_2O_4$ catalyst surface is not available for photon absorption[25]. Also, it noteworthy to mention that extra $Ag_{0.5}Zn_{0.5}Fe_2O_4$ catalyst concentration more than 40 mg/L, results in a shadowing effect and hinders the UV illumination to penetrate the aqueous mixture and thus reduces the oxidation rate[36,56].

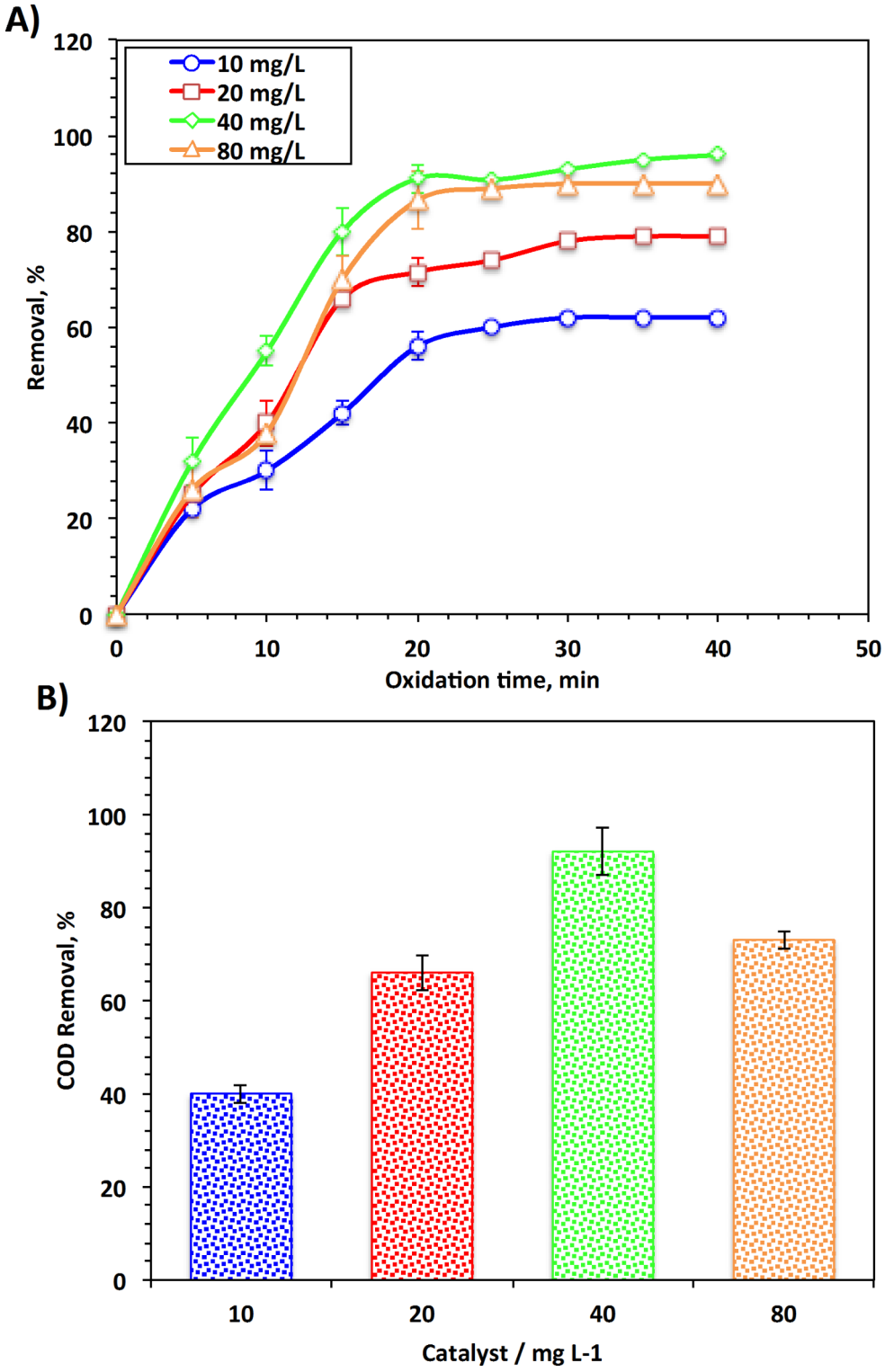

Fig. 8. Effect of catalyst loading on multiferroic-Fenton based oxidative system (H_2O_2 400 mg/L, pH 3.0).

Effect of multiferroic nanocomposite loading

For economic and more efficient feasibility, it is essential to locate the optimal catalyst dose. In an effort to reach to the adjusted reagent dosing for the concept of fitting the application, the catalyst ($Ag_{0.5}Zn_{0.5}Fe_2O_4$) loading is examined on the implementation of the photocatalytic oxidation system. In this concept, the concentration of $Ag_{0.5}Zn_{0.5}Fe_2O_4$ nanocomposite is assessed to explore Multiferroic-Fenton oxidation tendency (Fig. 8). The data exposed in Fig. 8 exhibits the effect of the Fenton oxidation on varies $Ag_{0.5}Zn_{0.5}Fe_2O_4$ from 10 to 80 in the units of mg per litre, whereas, all other operational variables are kept constant (400 mg/L for H_2O_2 and pH of 3.0).

The maximal Acinate removal efficacy is recorded to its almost complete (97%) removals as well as highest COD removal of 92% when 40 mg/L of catalyst is applied as a precursor of Multiferroic-Fenton system. While it reached to 62, 79 and 90% removals within the reaction time of 40 min, respectively for the corresponding doses of 10, 20 and 80 mg/L of $Ag_{0.5}Zn_{0.5}Fe_2O_4$, respectively. This might be validated through the amount of H_2O_2 of 400 mg/L, which is constant in all cases. Consequently, the achieved yield of ·OH radicals produced is not adequate reaching to a complete Acinate oxidation. Such investigation-attained means the H_2O_2 should be in balance to expand the (·OH) radicals' generation and could not be lessen the effective ·OH radicals' quantity. A comparable investigation is previously stated and reported in varied study[34,55]. This could be attributed by increasing the $Ag_{0.5}Zn_{0.5}Fe_2O_4$ catalyst concentration to more than the optimum value might leading to the affinity of the catalyst particles to agglomerate, therbey, part of the $Ag_{0.5}Zn_{0.5}Fe_2O_4$ catalyst surface is not available for photon absorption[25]. Also, it noteworthy to mention that extra $Ag_{0.5}Zn_{0.5}Fe_2O_4$ catalyst concentration more than 40 mg/L, results in a shadowing effect and hinders the UV illumination to penetrate the aqueous mixture and thus reduces the oxidation rate[36,56].

pH effectiveness on the multiferroic-Fenton system

Effectiveness of initial pH of the Acinate aqueous media is essential to investigate since the pH is valuable parameter in the Fenton reaction. Thus, pH is ranged from 3.0 to 8.0 whereas the 400 mg/L of hydrogen peroxide and 40 mg/L of $Ag_{0.5}Zn_{0.5}Fe_2O_4$ catalyst at the ultraviolet (UV) irradiance illumination. The results displayed in Fig. 9 exposed that the Acinate insecticide oxidation rate is enhanced by a decline in pH value to the acidic conditions. The optimal operational pH value recorded at 3.0. Nonetheless, rising the pH value results in a deterioration in the Acinate insecticide oxidation efficiency. Clearly, the alkaline pH value is critical since it regressions the OH radicals' generation and thereby declines the Acinate oxidation tendency and efficiency.

The pH effect on the Acinate oxidation system might be illustrated by the surface charge of $Ag_{0.5}Zn_{0.5}Fe_2O_4$ photocatalyst substance[13]. Thereby, changing in the medium pH reproduces a surface of the catalyst charge and thereby assumes the photo-catalytic affinity due to the electrostatic interactions[13,57]. At low substrate pH, the rate of generating ·OH radicals is high since the hydrogen peroxide decomposition rate is high whereas the ·OH radicals recombination reaction is minimal. Also, at acidic pHs, extra radicals are present in the reaction medium and on the catalyst surface compared to the basic medium, in this regard the pollutant are drawn closer to it by electrostatic gravitational forces, boosting their oxidation efficiency[20]. Moreover, the alkaline pH range might supports in the deprotonation of hydroxyl groups that declines the oxidation rate[36,58]. A similar investigation on oxidation of pharmaceutical discharge is reported using such reagent[20].

Temperature effect on kinetics and thermodynamics

It is important to validate the temperature consequence since it is an energetic influencing factor especially for the real practical application sector. Temperature affects the oxidation reaction efficiencies. Additionally, in real life, the disposed aqueous media of the solution mixture may be at various temperatures. From this regard, Acinate solution temperature is assorted from 28 to 60°C to evaluate the temperature outcome on the oxidation reaction.

The results of the experiments' data exhibited in Fig. 10 revealed a assumption in the Acinate oxidation reaction with the promotion in the solution temperature in the investigated range of the study. Approximately a complete (97%) Acinate insecticide removal is realized in about 60 min of reaction time at room temperature. Nonetheless, at higher temperature increase more than the room temperature (28°C), the proficiency is deteriorated. Notable, the optimum temperature is signified as 28 °C that accomplishing the best oxidation when compared with elevated temperature that is in accordance with the previous study reported in literature[38]. But, the overall yield of OH radicals is declined at high temperature that further reduces the Acinate oxidation. This might be elucidated by the high temperature delays the H_2O_2 decomposition for the generation of highly reactive species (·OH) radicals Additionally, extreme temperature of the aqueous solution decomposes hydrogen peroxide reagent into O_2 and H_2O, thereby, the outcome is a deduction in the overall attained oxidation[37–39].

The kinetics of oxidation is valuable estimation for the reactor design and the reaction control to reach to the real scale application that both affecting the processes efficiency and economic cost. Kinetic findings of this oxidation system are necessary to assess the complexity of intermediates generated in the reaction medium through the Multiferroic- Fenton based system. For further observing the oxidation test through the Multiferroic-Fenton Fenton system, the kinetics of the reaction is investigated. The kinetic study is investigated and the Acinate insecticide oxidation is inspected as a function of time and the data is fitted in the linearized integrated form of equations for both first and second order kinetic models according to the data tabulated in Table 1.

Based on the linearized form of kinetic rate equations, the kinetic rate constants of each model are then calculated and the results are tabulated in Table 1. Comparing the correlation coefficient values, R^2 projected from the plot of the linearized form equations estimating the best model fitted. Hence, the oxidation is following the first order reaction kinetics subsequently the correlation coefficient values are the uppermost (0.94–0.99) when it is compared to its corresponding values of the second order model. Also, the half reaction time life ($t_{1/2}$) is estimated and the data for the both models is displayed in Table 1. It is determined that the calculated $t_{1/2}$ value through first order kinetic equation was closely to experimental results. Previous work reported is in agreement with the current work[30,44–46].

In order to full understanding the Multiferroic-Fenton ($Ag_{0.5}Zn_{0.5}Fe_2O_4$) system, it is important to full study the temperature outcome on the system thermodynamics. The thermodynamic activation values of parameters are judged via the Arrhenius fit ($\ln k_1 = \ln A - \frac{E_a}{RT}$) that is based on the first order kinetic model due to its well fitted the data (*A* is pre-exponential factor, R is gas constants and *Ea* is the activation energy). First, the plot of plotting lnk_s versus 1/T offering a linear relation its slope estimates the activation energy (*Ea*). Subsequently,

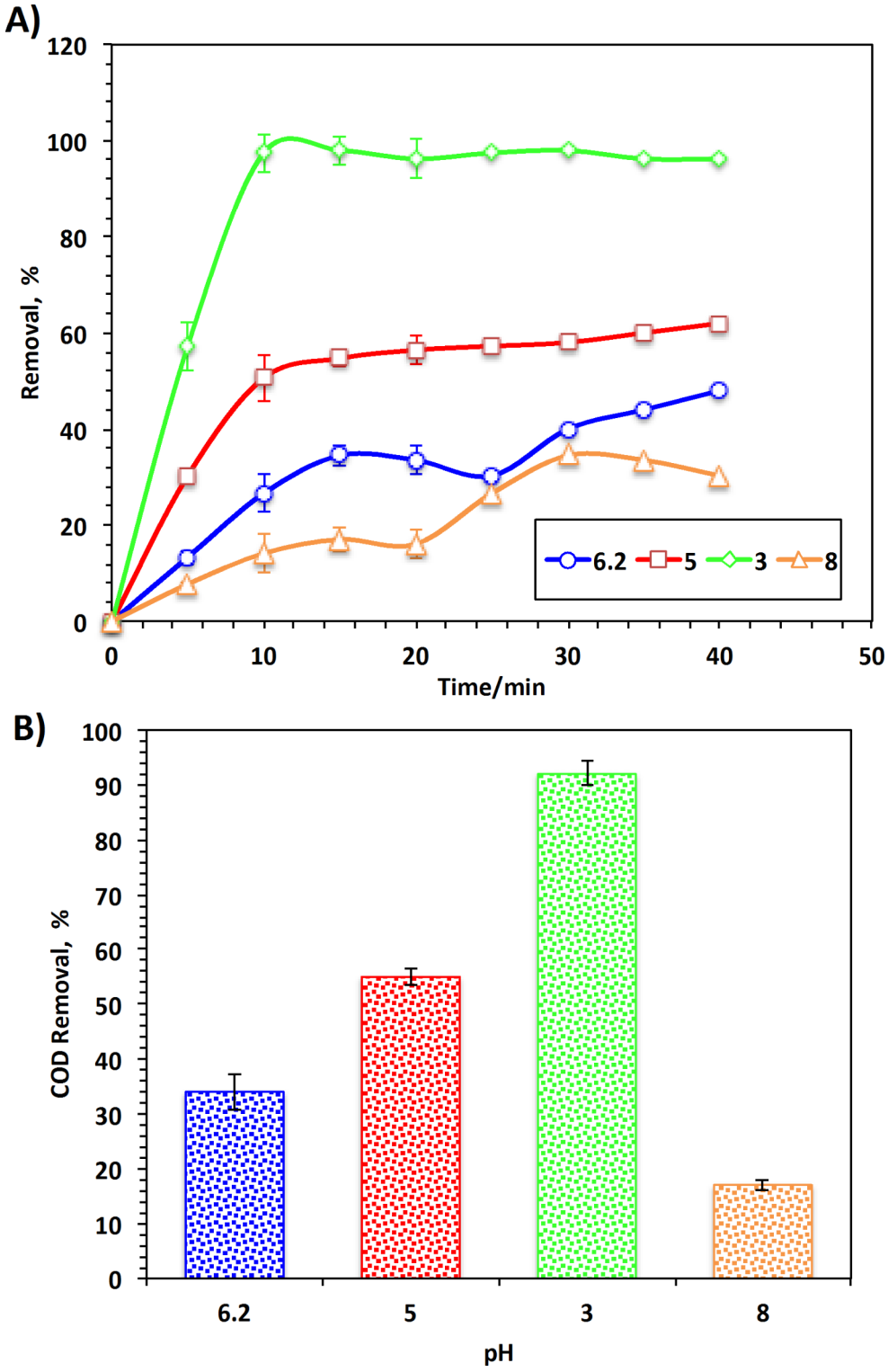

Fig. 9. Effect of solution pH on Multiferroic-Fenotn based oxidative system ($Ag_{0.5}Zn_{0.5}Fe_2O_4$ 40 mg/L and H_2O_2 400 mg/L).

Eyring equation ($k_2 = \frac{k_B T}{h} e^{(-\frac{\Delta G'}{RT})}$) ($k_B$ is Boltzmann and h is Planck's constants) is applied to investigate the other thermodynamic variables. Also, Enthalpy of activation ($\Delta H'$) ($\Delta H' = E_a - RT$) and the entropy of activation ($\Delta S'$) ($\Delta S' = (\Delta H' - \Delta G')/T$) is also estimated[47].

Additionally, Table 2 displayed the thermodynamic parameters data. The data recorded from such reaction tabulated in the Table reveals that the oxidation Multiferroic-Fenton ($Ag_{0.5}Zn_{0.5}Fe_2O_4$) system reacted in non-spontaneous manner since the Gibbs free energy of activation is positive, thereby this should mean the oxidation

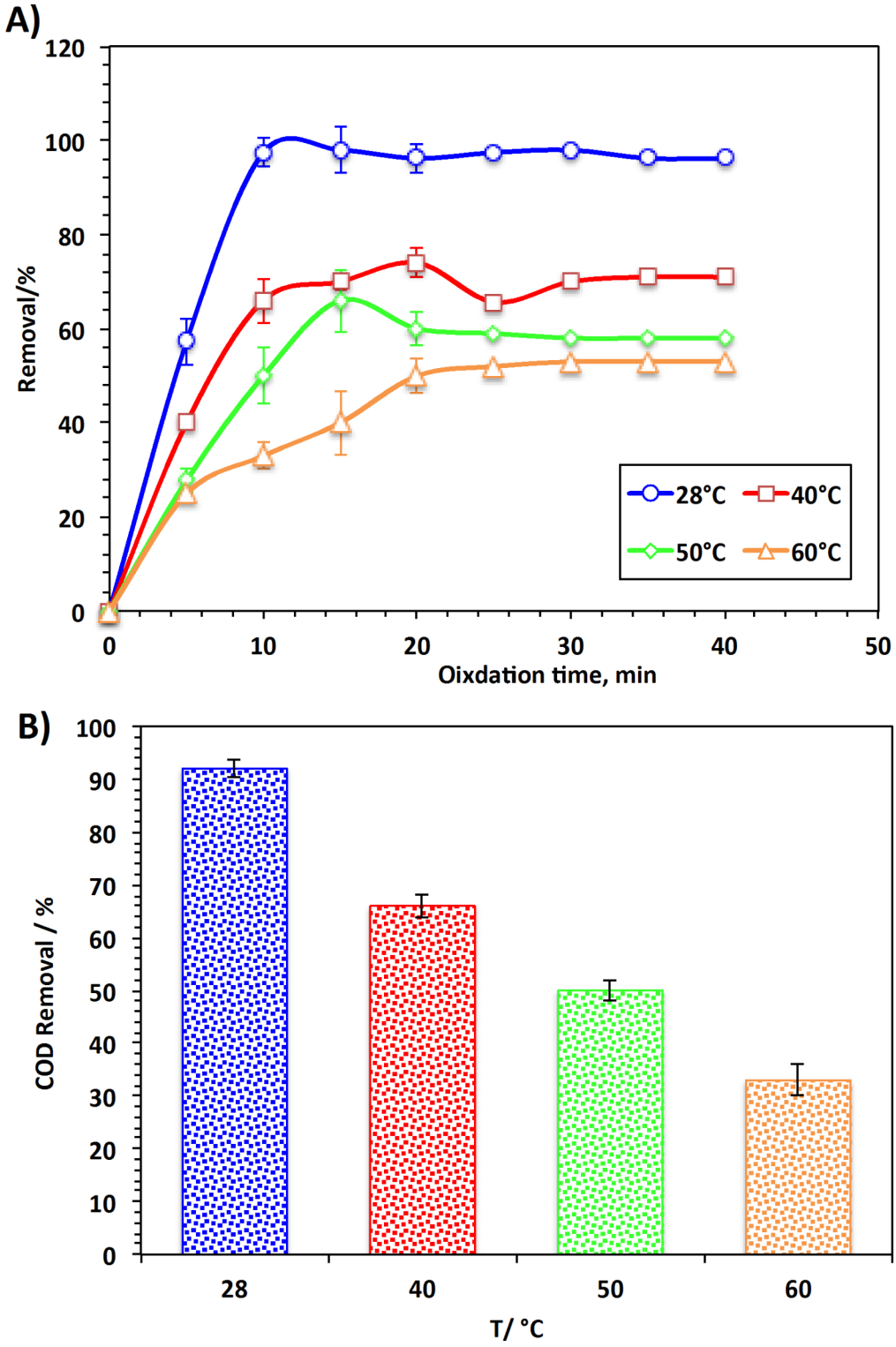

Fig. 10. Effect of temperature on multiferroic-Fenton based oxidative system ($Ag_{0.5}Zn_{0.5}Fe_2O_4$ 40 mg/L and H_2O_2 400 mg/L and pH 3.0).

is endergonic. This non-spontaneity is confirmed ΔS′ that posses a negative values and $\Delta H'$ that verified by their positive across all the studied temperatures. Negative gained values of entropy is due to the increase in randomness at the Acinate molecules as well as the produced hydroxyl radicals species[35]. The reaction is signified as an endothermic manner since $\Delta H'$ is greater than zero values and the ΔS′ shows a decline across the temperature elevation. This work is in agreement with the pervious recorded results cited in previously published articles[33–35].

Linearized kinetic model	Kinetic variables	Temperature, °C			
		28 °C	40 °C	50 °C	60 °C
Pseudo-first-order $(C_t = C_o - e^{k_1 t})$	k_1 (min^{-1})	0.30	0.17	0.11	0.08
	$t_{1/2}$ (min)	9.3	7.7	5.4	3.2
	R^2	0.94	0.98	0.99	0.98
Pseudo-second-order $\left(\left(\frac{1}{C_t}\right) = \left(\frac{1}{C_0}\right) - k_2 t\right)$	k_2 (L mg^{-1} min^{-1})	0.21	0.04	0.02	0.01
	$t_{1/2}$ (min)	0.31	1.51	5.32	7.51
	R^2	0.80	0.72	0.91	0.92

Table 1. Parameters of first- and second-kinetic models for Acinate removals through multiferroic-Fenton ($Ag_{0.5}Zn_{0.5}Fe_2O_4$) system.

Thermodynamic parameters	T/ °C			
	26 °C	40 °C	50 °C	60 °C
ΔH′ (kJ/mol)	77.03	80.22	86.41	90.03
ΔH′ (kJ/mol)	31.61	32.23	33.05	33.97
ΔS′ (J/mol K)	-147.72	-156.51	-176.05	-188.12
Ea (kJ/mol)	35.02			

Table 2. Thermodynamic parameters for Acinate insecticide oxidation by multiferroic-Fenton ($Ag_{0.5}Zn_{0.5}Fe_2O_4$) system.

Fenton type	Pollutant/concentration	Operating conditions	Oxidation (%)	Ref.
UV/Multiferroic $Ag_{0.5}Zn_{0.5}Fe_2O_4$	Actinate insecticide (20 mg/L)	$Ag_{0.5}Zn_{0.5}Fe_2O_4$ 40 mg/L; pH 3.0	97%	Current work
UV/Chitosan/Fe_3O_4	Methomyl insecticide (50 mg/L)	Chitosan/Fe_3O_4 3.0 g/L; pH 3.0	100%	
UV/Chitosan/ Fe_3O_4	Basic blue dye (10 mg/L)	Chitosan/Fe_3O_4; 2.4 mg/L; pH 7.0	100%	[8]
UV/$LaFeO_3$/BiOBr	Rhodamine B dye (5 mg/L)	$LaFeO_3$/BiOBr 0.1 gm	98.2%	[14]
UV/Titanium/iron oxides	Methyl Orange (80 mg/L)	Titanium/iron oxides 200 mg/L; pH 4.5	97%	[35]
Solar/Quartz/Hematite	Acinate insecticide (100 mg/L)	Quartz/Hematite 103 mg/L; pH 2.8	98%	[44]
Solar/Silver/Bismuth/iron oxides	Methyl Orange (40 mg/L)	Silver/Bismuth/iron oxides 0.6 g/L	97%	[11]
- UV/Fenton/Alumnium/Fe_3O_4	Methomyl pesticide (50 mg/L)	Aluminum/ Fe_3O_4 50 mg/L; pH 6.0	100%	[23]
Solar/Fenton-TiO_2@NH_2-MIL-88B(Fe)	Basic Blue 19 Dye (100 mg/L)	TiO_2@NH_2-MIL-88B(Fe) 200 mg/L; pH 7.0	100%	[35]
UV/sawdust-Fe_3O_4	Synozol Red dye (50 mg/L)	Sawdust -Fe_3O_4 1.0 g/ L; pH 3.0	99%	[45]
microwave Cu/C(II)/Cu(III)	Lannet insecticide (50 mg/L)	Cu/C(II)/Cu(III) 3.0 g/L; pH 6.5	91%	[43]
Solar/Magnetite-CeO_2-g-C_3N_4	tetracycline hydrochloride (50 mg/L)	Magnetite-CeO_2-g-C_3N_4 50 mg/L; pH 2.7	96.63%	[46]
UV/Fenton- alumnium/ Fe_3O_4	Levafix Blue Dye (50 mg/L)	Aluminum/ Fe_3O_4 2.0 g/L; pH 2.0	100%	[24]

Table 3. Fenton based system as comparative study of the work from the current investigation with corresponding in literature.

Comparative investigation

Table 3 displayed various Fenton system oxidation based systems from previous studies and compared them with the current examination. The study is based on modified Fenton system oxidation reaction and their effect on various pollutants to overcome the Fenton's limitations. The data in the pervious cited articles in literature are evaluated and compared with the current research. The comparative data reviewed in Table 3 showed the mixed cupper oxides are important to overcome the acidic pH conditions. Furthermore, other scattered authors used magnetite as a source of Fenton catalyst as a recyclable sustainable material. In comparison, the current work is based on using a superparamagnetic material to offers the reusable opportunity with minimal losses to highlight its environmentally benignity. Notable, minimum quaintly of catalyst in the present study is applied in comparison to the other work is signifying the consequence of the current investigated work as an economic material.

Recyclability of the multiferroic nanocatalyst

The recover and recycle ability of the Multiferroic nanocatalyst was evaluated by centrifuging the catalyst from the reaction heterogeneous mixture. The recovered catalyst was collected from the reaction medium and then reactive through successive washing with distilled water for introducing them for reuses facility. The reused Multiferroic nanocatalyst shoed a six times to oxidize Acinate solution. Figure 11 revealed that Ag@$ZnFe_2O_4$

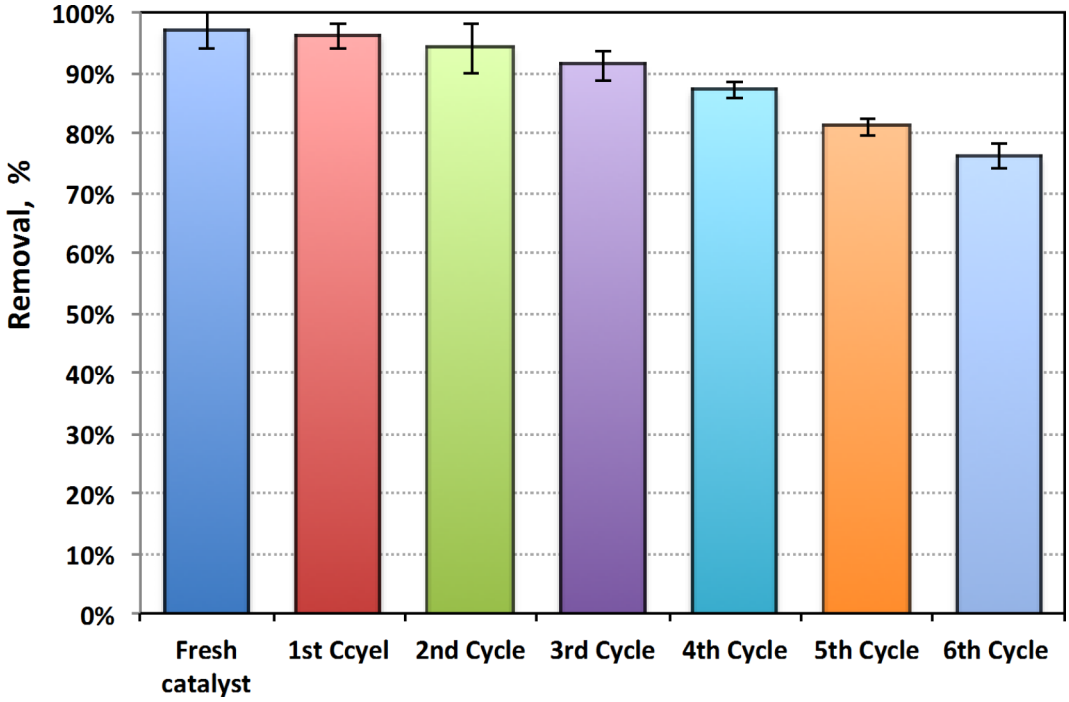

Fig. 11. Reusability of Multiferroic nanocatalyst for successive cycles.

nanocatalyst preserves its catalytic competence as a Fenton catalyst after six consecutive runs reached to 80% compared to 97% of the fresh use of experiments under UV irradiance for the purpose of Acinate oxidation. But, it is noteworthy to mention that the catalytic activity is a quite rendered than the fresh catalyst use due to the occupied Acinate molecules in the Multiferroic nanocatalyst. Overall, this study confirmed the Multiferroic material as a promising sustainable catalyst.

Conclusion

Multiferroic nanocatalyst tailored from multi nanoparticles, $Ag_{0.5}Zn_{0.5}Fe_2O_4$ is prepared by a simple co-precipitation route and used as a Fenton oxidation precursor. The morphological and structural analysis confirmed the Multiferroic nanocatalyst existence. The results showed 97% of Acinate insecticide removals within 40 min of irradiance time. The operating parameters are optimized and the optimal values are pH 3.0, hydrogen peroxide 400 mg/L and 40 mg/L of $Ag_{0.5}Zn_{0.5}Fe_2O_4$ nanocatalyst. The kinetic data confirmed the reaction is following e first order kinetic model reaction with minimal activation energy of 35.02 kJ/mol. Also, the sustainability of the catalyst is verified since its it showed a high oxidation efficiency even in the successive six cyclic use. Furthermore, such results will be leading for the application of such system in a pilot scale sunlight driven catalytic oxidation system treating a real wastewater sample.

Data availability

The data that support the findings of this study are available from the corresponding author upon reasonable request.

Received: 29 July 2024; Accepted: 4 November 2024
Published online: 07 November 2024

References

1. Abdollahzadeh, H. et al. Efficiency of activated carbon prepared from scrap tires magnetized by Fe_3O_4 nanoparticles: Characterisation and its application for removal of reactive blue19 from aquatic solutions. *Int. J. Environ. Anal. Chem.* https://doi.org/10.1080/03067319.2020.1745199 (2020).
2. Ahmadi, M., Behin, J. & Mahnam, A. R. Kinetics and thermodynamics of peroxydisulfate oxidation of reactive yellow 84. *J. Saudi Chem. Soci* **20**, 644–650 (2016).
3. Al Momani, F., Shawaqfah, M., Shawaqfeh, A. & Al-Shannag, M. Impact of Fenton and ozone on oxidation of wastewater containing nitroaromatic compounds. *J. Environ. Sci.* **20**, 675 (2008).
4. Argun, M. E. & Karatas, M. Application of Fenton process for decolorization of reactive black 5 from synthetic wastewater: Kinetics and thermodynamics. *Prog. Sust. Energy* **30**: 540 (2011).
5. Abdou, K. A., Mohammed, A. N., Moselhy, W. & Farghali, A. A. Assessment of modified rice husk and sawdust as bio-adsorbent for heavy metals removal using nano particles in fish farm. *Asian J. Anim. Vet. Adv.* **13**, 180–188 (2018).
6. Wulandari, I. O., Mardila, V. T., Santjojo, D. J. D. H. & Sabarudin, A. *Preparation and Characterization of Chitosan-Coated Fe_3O_4 Nanoparticles Using Ex-situ Co-precipitation Method and Tripolyphosphate/Sulphate as Dual Crosslinkers* vol. 299, 012064 (IOP Publishing).

7. Bia, X., Wanga, P., Jiao, C. & Cao, H. Degradation of remazol golden yellow dye wastewater in microwave enhanced ClO2 catalytic oxidation process. *J. Hazard. Mater.* **168**, 895–900 (2009).
8. Boretti, A. & Rosa, L. Reassessing the projections of the world water development report. *npj Clean. Water*. **2**, 15. https://doi.org/10.1038/s41545-019-0039-9 (2019).
9. Chen, R. & Pignatello, J. J. Role of quinone intermediates as electron shuttles in Fenton and photoassisted Fenton oxidations of aromatic compounds. *Environ. Sci. Technol.* **31**, 2399–2406 (1997).
10. Eltabey, M. M., Massoud, A. M. & Radu, C. Amendment of saturation magnetization, blocking temperature and particle size homogeneity in Mn-ferrite nanoparticles using co-zn substitution. *Mater. Chem. Phy*. **186**, 505–512 (2017).
11. Ercin, A. E. & Hoekstra, A. Y. Water footprint scenarios for 2050: A global analysis. *Environ. Inter.* **64**, 71–82 (2014).
12. Adesina, O. A., Abdulkareem, F., Yusuff, A. S., Lala, M. & Okewale, A. Response surface methodology approach to optimization of process parameter for coagulation process of surface water using Moringa oleifera seed. *S. Afr. J. Chem. Eng.* **28**, 46–51 (2019).
13. Rezgui, S. et al. $ZnFe_2O_4$-chitosan magnetic beads for the removal of chlordimeform by photo-Fenton process under UVC irradiation. *J. Environ. Manage.* **283**, 111987 (2021).
14. Ahmadi, M., Behin, J. & Mahnam, A. R. Kinetics and thermodynamics of peroxydisulfate oxidation of reactive yellow 84. *J. Saudi Chem. Soc.* **20**, 644–650 (2016).
15. Al, M. F., Mo'ayyad, S., Ahmad, S. & Mohammad, A-S. Impact of Fenton and ozone on oxidation of wastewater containing nitroaromatic compounds. *J. Environ. Sci.* **20**, 675–682 (2008).
16. Argun, M. E. & Karatas, M. Application of Fenton process for decolorization of reactive black 5 from synthetic wastewater: Kinetics and thermodynamics. *Environ. Prog. Sustain. Energy* **30**, 540–548 (2011).
17. Elsayed, S. A., El-Sayed, I. E. & Tony, M. A. Impregnated chitin biopolymer with magnetic nanoparticles to immobilize dye from aqueous media as a simple, rapid and efficient composite photocatalyst. *Appl. Water Sci.* **12**, 252. https://doi.org/10.1007/s13201-022-01776-3 (2022).
18. Bounab, L., Iglesias, O., González-Romero, E., Pazos, M. & Sanromán, M. Á. Effective heterogeneous electro-Fenton process of m-cresol with iron loaded actived carbon. *RSC Adv.* **5**, 31049–31056 (2015).
19. Clark, J. H., Farmer, T. J., Herrero-Davila, L. & Sherwood, J. Circular economy design considerations for research and process development in the chemical sciences. *Green Chem.* **18**, 3914–3934 (2016).
20. Rajabi, S. et al. Synergistic degradation of metronidazole and penicillin G in aqueous solutions using $AgZnFe_2O_4$@chitosan nano-photocatalyst under UV/persulfate activation. *Environ. Technol. Innov.* **35**, 103724 (2024).
21. El-Desoky, H. S., Ghoneim, M. M., El-Sheikh, R. & Zidan, N. M. Oxidation of Levafix CA reactive azo-dyes in industrial wastewater of textile dyeing by electro-generated Fenton's reagent. *J. Hazard. Mater.* **175**, 858–865 (2010).
22. Golka, K., Kopps, S. & Myslak, Z. W. Carcinogenicity of azo colorants: Influence of solubility and bioavailability. *Toxicol. Lett.* **151**, 203–210 (2004).
23. Guan, S., Yang, H., Sun, X. & Xian, T. Preparation and promising application of novel $LaFeO_3$/BiOBr heterojunction photocatalysts for photocatalytic and photo-Fenton removal of dyes. *Opt. Mater.* **100**, 109644 (2020).
24. Guan, X-H., Chen, G-H. & Shang, C. Re-use of water treatment works sludge to enhance particulate pollutant removal from sewage. *Water Res.* **39**, 3433–3440 (2005).
25. Karami, N. et al. Green synthesis of sustainable magnetic nanoparticles Fe_3O_4 and Fe_3O_4-chitosan derived from Prosopis farcta biomass extract and their performance in the sorption of lead (II). *Int. J. Biol. Macromol.* **254**, 127663 (2024).
26. Gharaghani, M. A. et al. Photocatalytic degradation of acid red 18 by synthesized $AgCoFe_2O_4$@ Ch/AC: Recyclable, environmentally friendly, chemically stable, and cost-effective magnetic nano hybrid catalyst. *Int. J. Biol. Macromol.* **269**, 131897 (2024).
27. Mohammadpour, A. et al. Green synthesis, characterization, and application of Fe_3O_4 nanoparticles for methylene blue removal: RSM optimization, kinetic, isothermal studies, and molecular simulation. *Environ. Res.* **225**, 115507 (2023).
28. Laib, S., Rezzaz-Yazid, H., Yatmaz, H. C. & Sadaoui, Z. *Low Cost Effective Heterogeneous Photo-Fenton Catalyst from Drinking Water Treatment Residuals for Reactive Blue 19 Degradation: Preparation and Characterization* (Water Environment Research, 2021).
29. Li, X., Cui, J. & Pei, Y. Granulation of drinking water treatment residuals as applicable media for phosphorus removal. *J. Environ. Manage.* **213**, 36–46 (2018a).
30. Li, Y. et al. TiO_2 nanoparticles anchored onto the metal–organic framework NH2-MIL-88B (Fe) as an adsorptive photocatalyst with enhanced fenton-like degradation of organic pollutants under visible light irradiation. *ACS Sustain. Chem. Eng.* **6**, 16186–16197 (2018b).
31. Muthukannan, V., Praveen, K. & Natesan, B. Fabrication and characterization of magnetite/reduced graphene oxide composite incurred from iron ore tailings for high performance application. *Mater. Chem. Phys.* **162**, 400–407 (2015).
32. Tandon, R., Tandon, N. & Patil, S. M. Overview on magnetically recyclable ferrite nanoparticles: Synthesis and their applications in coupling and multicomponent reactions. *RSC Adv.* **11**, 29333 (2021).
33. Oyewo, O. A., Adeniyi, A., Sithole, B. B. & Onyango, M. S. Sawdust-based cellulose nanocrystals incorporated with ZnO nanoparticles as efficient adsorption media in the removal of methylene blue dye. *ACS Omega*. **5**, 18798–18807 (2020).
34. Pourali, P. et al. Removal of acid blue 113 from aqueous solutions using low-cost adsorbent: adsorption isotherms, thermodynamics, kinetics and regeneration studies. *Sep. Sci. Technol.* 1–13 (2021).
35. Sharma, R., Bansalb, S. & Sonal Singh, S. Tailoring the photo-Fenton activity of spinel ferrites (MFe_2O_4) by incorporating different cations (M ¼ Cu, Zn, Ni and Co) in the structur. *RSC Adv.* **5**, 6006 (2015).
36. Thabet, R. H., Fouad, M. K., Ali, I. A., El Sherbiney, S. A. & Tony, M. A. Magnetite-based nanoparticles as an efficient hybrid heterogeneous adsorption/oxidation process for reactive textile dye removal from wastewater matrix. *Int. J. Environ. Anal. Chem.* 1–23 (2021).
37. Patil, S., Bedre, A., Gade, V., Jopale, M. & Pise, A. One-pot protocol for the reductive amination of aldehydes using thiamine hydrochloride as a green catalyst under solvent-free condition. *Synth. Commun.* **53**(18), 1545–1558. https://doi.org/10.1080/00397911.2023.2236258 (2023).
38. Patil, S. M. R. & Bedre, A. V. Recent progress in Fe_3O_4 nanoparticles and their green applications in organic transformations. *Iran. J. Catal.* **13**(3), 235–270 (2023).
39. Rao, T. K. Synthesis and characterization of zinc oxide @ silver ferrite multiferroic nanocomposite. *Mater. Today: Proc.* **46**, 10747–10751 (2021).
40. Patil, S. M., Tandon, R. & Tandon, N. Magnetically recoverable silica-decorated ferromagnetic-nanoceria nanocatalysts and their use with *O*- and *N*-butyloxycarbonylation reaction via solvent-free condition. *ACS Omega*. **7** (28), 24190–24201 (2022).
41. Abdel Maksoud, M. A., El-Sayyad, G. S., El-Bastawisy, H. S. Fathy, R. M. Antibacterial and antibiofilm activities of silverdecorated zinc ferrite nanoparticles synthesized by a gamma irradiation-coupled sol–gel method against some pathogenic bacteria from medical operating room surfaces. *RSC Adv.* **11**, 28361 (2021).
42. Thabet, R. H., Fouad, M. K., El Sherbiney, S. A. & Tony, M. A. Solar assisted green photocatalysis for deducing carbamate insecticide from agriculture stream into water reclaiming opportunity. *Int. J. Environ. Anal. Chem.* 1–23 (2022).
43. Thabet, R. H., Fouad, M. K., Sherbiny, S. A. E. & Tony, M. A. Zero-waste approach: Assessment of aluminum-based waste as a photocatalyst for industrial wastewater treatment ecology. *Int. J. Environ. Res.* **16**, 1–19 (2022b).
44. Xu, Z. et al. Visible light-degradation of azo dye methyl orange using TiO_2/β-FeOOH as a heterogeneous photo-Fenton-like catalyst. *Water Sci. Technol.* **68**, 2178–2185 (2013).

45. Tony, M. A. & Lin, L.-S. Iron coated-sand from acid mine drainage waste for being a catalytic oxidant towards municipal wastewater remediation. *Int. J. Environ. Res.* 1–11 (2021).
46. Soliman, E. M., Ahmed, S. A. & Fadl, A. A. Adsorptive removal of oil spill from sea water surface using magnetic wood sawdust as a novel nano-composite synthesized via microwave approach. *J. Environ. Health Sci. Eng.* **18**, 79–90 (2020).
47. Patil, S. M., Ingale, A. P., Pise, A. S. & Bhondave, R. S. Novel cobalt-supported silica-coated ferrite nanoparticles applicable for Acylation of amine, phenol, and thiols derivatives under Solvent-free condition. *Materials Science inc. Nanomaterials & Polymers, ChemistrySelect* **7**, e202201590 (1 of 9) (2022).
48. Patil, S. M., Tandon, R., Tandon, N., Singh, I., Bedreb, A. & Gadec, V. Magnetite-supported montmorillonite (K10) (nanocat-Fe-Si-K10): an efficient green catalyst for multicomponent synthesis of amidoalkyl naphthol. *RSC Adv.* **13**, 17051 (2023).
49. Ingale, A. Catalyst-free, efficient and one pot protocol for synthesis of nitriles from aldehydes using glycerol as green solvent. *Tetrahedron Letters* (2017).
50. Pise, A., Patil, S. M. & Ingale, A. P. Malic acid as a green catalyst for the N-Boc protection under Solvent-free condition. https://doi.org/10.2174/0115701786278928231218113855
51. Thabet, R. H., Tony, M. A., El Sherbiny, S. A., Ali, I. A. & Fouad, M. K. Catalytic oxidation over nanostructured heterogeneous process as an effective tool for environmental remediation. *IOP Conf. Series: Mater. Sci. Eng.* **975**, 012004 (2020).
52. Wang, S. et al. Magnetic $Fe_3O_4/CeO_2/g\text{-}C_3N_4$ composites with a visible-light response as a high efficiency Fenton photocatalyst to synergistically degrade tetracycline. *Sep. Purif. Technol.* **278**, 119609 (2021).
53. Patil, S., Tandon, R. & Tandon, N. A current research on silica coated ferrite nanoparticle and their application: review. *Curr. Res. Green. Sustainable Chem.* **4**, 100063 (2021).
54. Tandon, N., Patil, S. M., Tandon, R. & Kumar, P. Magnetically recyclable silica-coated ferrite magnetite-K10 montmorillonite nanocatalyst and its applications in O, N, and S-acylation reaction under solvent-free conditions. *RSC Adv.* **11**, 21291 (2021).
55. Patil, S. M., Tandon, R. & Tandon, N. Synthesis and characterization of $Fe_3O_4@SiO_2@K_{10}$ NPs applicable for N-ter-butyloxycarbonylation using solvent-free conditions. *Journal of Physics: Conference Series* **2267**, 012107 (2022).
56. Tandon, R., Patil, S., Tandon, N. & Kumar, P. Magnetically recyclable silica-coated Magnetite-Molybdate Nanocatalyst and its applications in N-Formylation reactions under solvent-free conditions. *Lett. Org. Chem.* **19** (8), 616–626 (2022).
57. Pise, A. S., Ingale, A. P. & Patil, S. M. An efficient synthesis of 1, 3-oxazine derivatives catalyzed under ceric ammonium nitrate in an aqueous medium at ambient temperature. *Polycyclic Aromatic Compounds* https://doi.org/10.1080/10406638.2023.2259569 (2023).
58. Vavilapalli, D. S., Srikanti, K., Mannam, R., Tiwari, B. & Mohan Kant, K., Ramachandra Rao, M. S. & Singh, S. Photoactive brownmillerite multiferroic $KBiFe_2O_5$ and its potential application in sunlight-driven photocatalysis. *ACS Omega* **3**, 16643–16650 (2018).

Acknowledgements

The authors extend their appreciation to Prince Sattam bin Abdulaziz University for funding this research work through the project number (PSAU/2024/01/921606).

Author contributions

Conceptualization, M.A.T.; Methodology, H.A.N. and M.A.T.; Software, H.A.N.; investigation, H.A.N.; Writing—Original Draft, H.A.N. and M.A.T.; Writing—Review and Editing, H.A.N.; Project Administration, H.A.N. All authors reviewed the manuscript.

Declarations

Competing interests

The authors declare no competing interests.

Additional information

Correspondence and requests for materials should be addressed to H.A.N.

Reprints and permissions information is available at www.nature.com/reprints.

Publisher's note Springer Nature remains neutral with regard to jurisdictional claims in published maps and institutional affiliations.